Substitution of an Active Site Valine Uncovers a Kinetically Slow Equilibrium between Competent and Incompetent Forms of Choline Oxidase[†]

Steffan Finnegan[‡] and Giovanni Gadda*[,‡,§,||]

Departments of Chemistry and Biology, The Center for Biotechnology and Drug Design, Georgia State University, Atlanta, Georgia 30302-4098

Received July 30, 2008; Revised Manuscript Received October 15, 2008

ABSTRACT: The enzymatic oxidation of choline to glycine betaine is of interest because organisms accumulate glycine betaine intracellularly in response to stress conditions. This is relevant for the genetic engineering of crops with economic interest that do not naturally possess efficient pathways for the synthesis of glycine betaine and for the potential development of drugs that target the glycine betaine biosynthetic pathway in human pathogens. To date, the best characterized choline-oxidizing enzyme is the flavin-dependent choline oxidase from *Arthrobacter globiformis*, for which structural, mechanistic, and biochemical data are available. Here, we have replaced a hydrophobic residue (Val464) lining the active site cavity close to the N(5) atom of the flavin with threonine or alanine to investigate its role in the reaction of choline oxidation catalyzed by choline oxidase. The reductive half-reactions of the enzyme variants containing Thr464 or Ala464 were investigated using substrate and solvent kinetic isotope effects, solvent viscosity effects, and proton inventories. Replacement of Val464 with threonine or alanine uncovered a kinetically slow equilibrium between a catalytically incompetent form of enzyme and an active species that can efficiently oxidize choline. In both variants, the active form of enzyme shows a decreased rate of hydroxyl proton abstraction from the alcohol substrate, with minimal changes in the subsequent rate of hydride ion transfer to the flavin. This study therefore establishes that a hydrophobic residue not directly participating in catalysis plays important roles in the reaction of choline oxidation catalyzed by choline oxidase.

The four-electron, enzymatic oxidation of choline to glycine betaine (*N,N,N*-trimethylglycine) is of considerable interest because glycine betaine is a biocompatible solute that is accumulated in the cytoplasm of prokaryotic and eukaryotic organisms as a defensive mechanism to counteract deleterious stresses, such as extreme temperature changes or high osmotic pressures (*1*−*5*). This has significant relevance for the genetic engineering of specific stress tolerant crops of economic interest such as tomato and rice that, by virtue of having inefficient biosynthetic pathways for the production of glycine betaine, are particularly vulnerable to stress conditions (*6*−*13*). Amassing large amounts of glycine betaine in the cytoplasm is particularly critical for bacteria, where adjustment of the cellular water content is attained by controlling the level of the intracellular solute pool due to lack of active water transport systems (*3, 5*). Failure to do so in hyperosmotic environments immediately triggers fluxes of water across the cytoplasmic membrane resulting in dehydration and plasmolysis. Choline and its precursors phosphatidyl choline, phosphocholine and acetylcholine are very abundant at infection sites (*14*−*16*), where osmotic stress conditions are frequently observed (*17*). In a number of human pathogens, including *Pseudomonas aeruginosa*, *Listeria monocytogenes*, *Vibrio cholerae*, *Enterococcus faecalis*, *Klebsiella pneumoniae*, or urophatogenic *Escherichia coli*, glycine betaine accumulates in the cytoplasm and allows growth in hyperosmotic minimal media of clinical isolates (*18*−*22*). Moreover, physiological responses to osmotic stress have recently gained attention with several studies showing that high osmolarity is one of the major environmental signals controlling the expression of genes associated with cellular invasion and virulence in a variety of human pathogenic microorganisms (*23*−*29*). In the model organism *E. coli*, the expression of a membrane-associated flavin-dependent, choline-oxidizing enzyme and a choline transporter for the production of glycine betaine are immediately up-regulated in media with high osmolality (*30, 31*). Regulation of intracellular osmolality to hyperosmotic environments is also intimately connected to a number of physiological responses, such as increased heat and cold tolerance, and regulation of the internal pH and ionic strength (*6, 9, 32*−*35*). Consequently, the study of the biophysical and mechanistic properties of flavin-dependent, choline-oxidizing enzymes has potential for the development of therapeutic agents that inhibit the biosynthesis of glycine betaine and render the bacteria either more susceptible to the immune system or to conventional treatments with antibiotics.

[†] This work was supported in part by grants from NSF-CAREER MCB-0545712 (to G.G.) and an MBD-Fellowship from Georgia State University (to S.F.).

* To whom correspondence should be addressed. Department of Chemistry, Georgia State University, P.O. Box 4098, Atlanta, GA 30302-4098. Phone: (404) 413-5537. Fax: (404) 413-5505. E-mail: ggadda@gsu.edu.

[‡] Department of Chemistry.

[§] Department of Biology.

[||] The Center for Biotechnology and Drug Design.

10.1021/bi801424p CCC: $40.75 © 2008 American Chemical Society
Published on Web 12/03/2008

Scheme 1: Flavin-Mediated, Four-Electron Oxidation of Choline to Glycine Betaine Catalyzed by Choline Oxidase

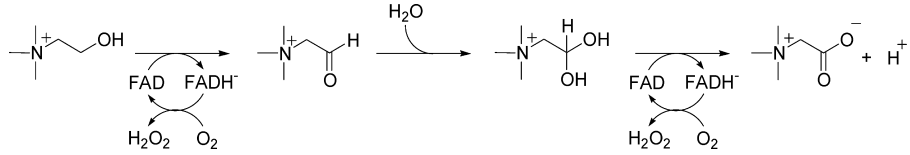

Scheme 2: Hydride Transfer Mechanism for the Oxidation of Choline to Betaine Aldehyde Catalyzed by Choline Oxidase

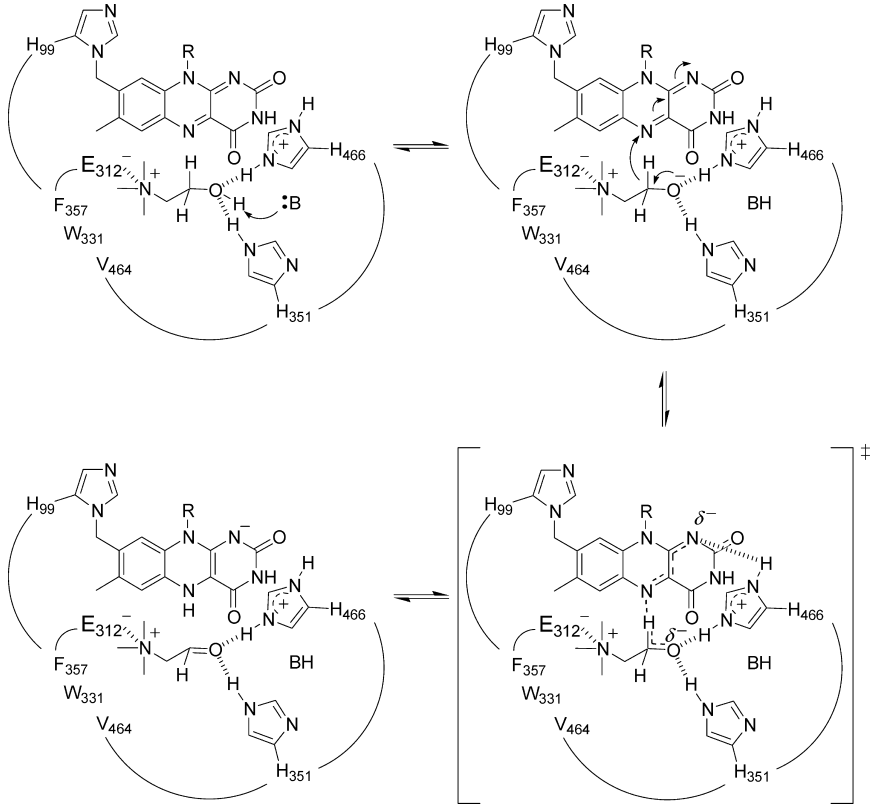

Two types of flavin-containing choline-oxidizing enzymes have been identified to date: a cytosolic, soluble choline oxidase (*36*−*38*) and a membrane-associated choline dehydrogenase (*21, 39*−*41*). These enzymes catalyze the identical oxidation of choline to glycine betaine via betaine aldehyde as intermediate, but prefer different primary electron acceptors (see Scheme 1 for the reaction catalyzed by choline oxidase). Indeed, the classification of the two enzymes is based on initial reports showing that choline oxidase readily reacts with O_2 (*42*), while choline dehydrogenase prefers electron acceptors other than O_2 (*43, 44*). Difficulties of keeping choline dehydrogenase stable and active after extraction from its cellular source have hindered an in depth biochemical characterization of the enzyme (*43, 44*). In contrast, due to the obtainment of large amounts of soluble, stable, and active choline oxidase, significant progress in the understanding of the mechanistic, biochemical, and structural properties of the flavin-dependent choline-oxidizing enzymes has been achieved (*42, 45*−*56*).

The reductive half-reaction in which choline is oxidized to betaine aldehyde in choline oxidase has been characterized in detail in the wild-type enzyme (*42, 45*−*56*). The reaction is initiated in the enzyme−substrate Michaelis complex by the removal of the hydroxyl proton of the alcohol substrate (Scheme 2), as suggested by kinetic isotope effects (*42, 47*). Stabilization of the resulting choline alkoxide species is provided by the side chains of His351, His466, and Glu312 (*49, 54, 55*). These electrostatic and hydrogen bonding interactions, along with the limited mobility of the flavin cofactor that is covalently linked through its C(8) methyl group to His99 (*54*), are major contributors to the preorganization of the enzyme−substrate complex for an efficient oxidation reaction (*54*). Once activation and stabilization of the alkoxide species are achieved, a hydride ion tunnels from the alkoxide α-carbon to the N(5) atom of the flavin as a result of environmental vibrations of the reaction coordinate that permit a tunneling distance between the hydride donor and acceptor (*48*). The hydride donor and acceptor are brought in a configuration compatible with environmentally assisted tunneling through a conformational change of the enzyme−substrate complex that is mechanistically and kinetically distinct from the hydride transfer reaction, as suggested by temperature-dependent studies on the reaction catalyzed by the wild-type enzyme under reversible and irreversible catalytic regimes (*48, 53*). Such a conformational change of the enzyme−substrate complex is also observed upon replacing the side chain of Glu312, which is important for the binding and positioning of the alcohol substrate in the active site of the enzyme, with an aspartate residue (*54*).

In the three-dimensional structure of choline oxidase recently solved to a resolution of 1.86 Å (*54*), the hydrophobic residue Val464 lines the active site cavity in proximity of the N(5) atom of the isoalloxazine ring of the flavin

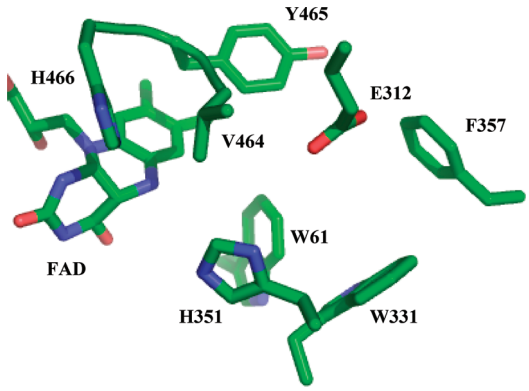

FIGURE 1: Close-up view of the active site of the wild-type form of choline oxidase showing the positioning of Val464 with respect to the isoalloxazine ring of the flavin and the active site cavity (PDB entry 2jbv). Note the distortion of the flavin ring, which is due to the presence of a C(4a) flavin adduct (not shown here), whose identity is currently being investigated.

cofactor, with its side chain establishing a van der Waals contact with the C(2) atom of the conserved His466 (Figure 1). Such an arrangement suggests that, although Val464 does not directly participate in the reaction of choline oxidation catalyzed by the enzyme, it may play an important role in catalysis. In this study, the effects of replacing Val464 with a hydrophilic residue (Thr) or an amino acid with a shorter side chain (Ala) on the hydrophobic packing needed for proper organization of the active site in the reductive half-reaction catalyzed by choline oxidase have been investigated. The enzyme variants Val464Thr[1] and Val464Ala were prepared using site-directed mutagenesis and purified to homogeneity using ion exchange chromatography. The reductive half-reactions with choline as anaerobic substrate for the enzyme variants were investigated using an array of mechanistic probes including substrate and solvent kinetic isotope effects, solvent viscosity effects, and proton inventories. The results presented uncovered a kinetically slow equilibrium involving a catalytically incompetent form of enzyme and an active species that oxidizes choline. The active form of both enzyme variants showed lower rates of hydroxyl proton abstraction from the alcohol substrate as compared to the wild-type enzyme, with minimal effects on the rates of the subsequent hydride transfer reaction.

EXPERIMENTAL PROCEDURES

Materials. Strain Rosetta(DE3)pLysS of *Escherichia coli* was from Novagen (Madison, WI). DNase was from Roche (Indianapolis, IN). The QuikChange site-directed mutagenesis kit was from Stratagene (La Jolla, CA). The QIAprep Spin Miniprep kit was from Qiagen (Valencia, CA). Oligonucleotides used for sequencing of the mutant genes were custom synthesized by Sigma Genosys (Woodland, TX). Choline chloride was from ICN Pharmaceutical Inc. (Irvine, CA); 1,2-[$^2H_4$]-choline bromide (98%) and sodium deuterium oxide (99%) were from Isotec Inc. (Miamisburg, OH); glucose and glucose oxidase were from Sigma (St. Louis, MO); and Polyethylene glycol 6000 was from Fluka (St. Louis, MO). All other reagents were of the highest purity commercially available.

Site-Directed Mutagenesis. The variant forms of choline oxidase Val464Ala and Val464Thr were prepared using the pET/codAmg plasmid harboring the wild-type gene for choline oxidase as template for site-directed mutagenesis, as previously described (*45, 52, 54*). The presence of the desired mutations was confirmed by sequencing the entire mutagenized genes. *E. coli* strain Rosetta(DE3)pLysS competent cells were transformed with the mutant plasmids by electroporation. Host cells not containing the mutant plasmid showed no enzymatic activity with choline as a substrate.

Expression and Purification of the Val464Ala and Val464Thr Variants of Choline Oxidase. The mutant enzymes were expressed and purified to homogeneity using the same procedure described previously for the purification of the wild-type enzyme (*45, 46*). Typically, between 600 and 700 mg of purified enzymes were obtained from 5 L of cell culture. The enzymes maintained full enzymatic activity for at least six months upon storage in 20 mM Tris-Cl, pH 8, at −20 °C.

Spectroscopic Studies. The pH dependence of the UV−visible absorbance spectra for the Val464 variant enzymes were determined by titrating with sodium hydroxide as previously described for the His466Ala mutant enzyme (*49*).

Enzyme Assays. Presteady-state kinetic measurements were carried out using an SF-61DX2 HI-TECH KinetAsyst high performance stopped-flow spectrophotometer thermostatted at 25 °C, in 50 mM sodium pyrophosphate, pH 10. The rate of flavin reduction was measured by monitoring the decrease in absorbance at 455 nm that results from the anaerobic mixing of choline oxidase with the organic substrate as previously described for the wild-type enzyme (*47*), except that 5 mM glucose and 0.5 μM glucose oxidase were present to scavenge possible trace amounts of oxygen. After anaerobic mixing in the stopped-flow spectrophotometer, the final concentration of the enzymes was ~10 μM, whereas those of the organic substrates were between 0.05 to 10 mM, thereby maintaining pseudo-first-order kinetic conditions. For the determination of the solvent kinetic isotope effects on the rate of flavin reduction, all of the reagents were prepared as described above except that D_2O was used to dissolve both the enzymes and substrates, and the pH of the buffered solution containing the enzyme was adjusted to 9.6 to account for the isotope effect on the ionization of sodium pyrophosphate (*57*). Solvent viscosity effects were measured in the presence of 8% (v/v) glucose or 0.0211 g/mL PEG-6000 as viscosigens, in both the tonometer containing the enzyme and the syringes containing the organic substrates. The resulting relative viscosities at 25 °C were 1.25 and 1.26 for glucose and PEG-6000 respectively, slightly above the value of 1.23 representing a 100% solution of D_2O (*58, 59*). For proton inventories in solvents containing varying mole fractions of D_2O, the pD values were adjusted using DCl and NaOD based on the empirical relationship (eq 1) that exists between the pH-meter reading and the pD value at varying mole fractions of D_2O (n) (*57*). For each concentration of substrate, the rates of flavin reduction were recorded in triplicate, with measurements differing by ≤5%.

$$(\Delta pH)_n = 0.076n^2 + 0.3314n \quad (1)$$

[1] Abbreviations: Val464Ala, choline oxidase variant with valine 464 replaced with alanine; Val464Thr, choline oxidase variant with valine 464 replaced with threonine; His466Ala, choline oxidase variant with histidine 466 replaced with alanine.

Scheme 3: Proposed Kinetic Mechanism for Choline Oxidation Catalyzed by the Val464Thr and Val464Ala Enzymes[a]

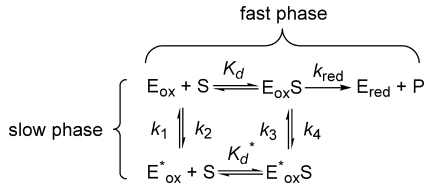

[a] E_{ox}, catalytically competent enzyme; E^*_{ox}, catalytically incompetent enzyme; S, substrate; k_{red}, first-order rate constant for flavin reduction; K_d, macroscopic dissociation constant for substrate binding to the competent enzyme; K_d^*, macroscopic dissociation constant for substrate binding to the incompetent enzyme; k_1 and k_3, first-order rate constants for the conversion of catalytically inert to competent enzyme; k_2 and k_4, first-order rate constants for the conversion of catalytically competent to inert enzyme.

Data Analysis. Kinetic data were fit with KaleidaGraph (Synergy Software, Reading, PA) and the Hi-Kinetic Studio Software Suite (Hi-Tech Scientific, Bradford on Avon, U.K.). Stopped-flow data traces were fit with eq 2, which describes a double-exponential process, in which k_{obs1} and k_{obs2} are the observed rate constants for the change in absorbance at 455 nm, A is the value of absorbance at time t, B and C are the amplitudes of the absorbance changes for the fast and slow observed phases, respectively, and D is an offset value that accounts for the nonzero absorbance value at infinite time. Presteady-state kinetic parameters were determined by using eqs 3 and 4, which apply to the kinetic mechanism of Scheme 3 (see Results). In eq 3, k_{obs1} is the observed first-order rate constant associated with the fast phase of flavin reduction at any given concentration of substrate, k_{red} is the limiting first-order rate constant for flavin reduction at saturating substrate concentrations, S is substrate concentration, and K_d is the macroscopic dissociation constant for binding of the substrate to the active enzyme. In eq 4, k_{obs2} is the observed first-order rate constant associated with the slow phase of flavin reduction at any given concentration of substrate, k_1 is the first-order rate constant for the conversion of the E^*_{ox} to E_{ox}, k_3 is the first-order rate constant for the conversion of $E^*_{ox}S$ to $E_{ox}S$, K_d^* represents the macroscopic dissociation constant for binding of the substrate to the incompetent enzyme, and S is substrate concentration (see Appendix for derivation of eq 4) (*60, 61*). Data for the pH dependence of the UV−visible absorbance spectra were fit to eq 5, which describes a curve with two plateau regions at low (Y_L) and high (Y_H) pH connected by a decrease in absorbance with a slope of −1 followed by an increase with a slope of +1.

$$A = B\exp(-k_{obs1}t) + C\exp(-k_{obs2}t) + D \quad (2)$$

$$k_{obs1} = \frac{k_{red}S}{K_d + S} \quad (3)$$

$$k_{obs2} = \left(\frac{k_3S + k_1K_d^*}{S + K_d^*}\right) \quad (4)$$

$$Y = \frac{(Y_L \times 10^{-pK_{a1}} + Y_H \times 10^{-pH})}{(10^{-pK_{a1}} + 10^{-pH})} + \frac{(Y_H \times 10^{-pK_{a2}} + Y_L \times 10^{-pH})}{(10^{-pK_{a2}} + 10^{-pH})} \quad (5)$$

RESULTS

Purification of the Val464Ala and Val464Thr Enzymes. Two variant forms of choline oxidase were engineered using site-directed mutagenesis to replace a valine at position 464 with alanine or threonine. The enzymes were independently expressed in *E. coli* strain Rosetta(DE3)pLysS and purified by following the same protocol established for the wild-type enzyme (*45*). Upon purification, the variant enzymes displayed a covalently bound flavin cofactor in the form of a nonreactive, air-stable, anionic flavosemiquinone (data not shown). The fully oxidized forms of the enzymes were obtained via slow oxidation of the flavosemiquinone by extensive dialysis at pH 6 and 4 °C, as previously reported for the wild-type and a number of active site mutant forms of choline oxidase (*42, 54, 55*). The specific activities of the resulting fully oxidized forms of the Val464Ala and Val464Thr enzymes were 0.3 μmol O_2 $min^{-1}mg^{-1}$ with 10 mM choline as substrate at pH 7. This value corresponds to a 25-fold decrease with respect to the specific activity of the wild-type enzyme (with a value of 8 μmol O_2 $min^{-1}mg^{-1}$) (*54*), suggesting that Val464 is an important residue for catalysis in choline oxidase.

Reductive Half-Reaction with Choline. The reductive half-reaction in which the Val464Ala or Val464Thr enzymes are reduced anaerobically with the substrate was investigated using a stopped-flow spectrophotometer by measuring the rates of decrease in absorbance at 455 nm as a function of the concentration of choline in 50 mM sodium pyrophosphate, pH 10, and 25 °C, under pseudo-first-order conditions (i.e., 10 μM enzyme and ≥50 μM substrate). pH 10 has previously been shown to be in the pH independent region for the wild type as well as for various mutant forms of choline oxidase (*42, 49, 54, 55*). As illustrated in the examples of Figures 2A and S1 (Supporting Information), both investigated variant enzymes were reduced to the hydroquinone state in a biphasic pattern, with a fast phase accounting for approximately 60 to 70% of the total change in absorbance, contrary to the monophasic reduction observed for the wild type enzyme (*47*). The relative amplitudes of the kinetic phases seen in the stopped-flow traces were independent of the concentration and the isotopic composition of the substrate, as similar results were obtained with 1,2-[$^2H_4$]-choline (Figures 2A and S1 insets (Supporting Information)), indicating that the kinetic behavior displayed by the Val464 variants is an intrinsic property of the enzymes that is unrelated to the substrate. The reductive half-reaction of the Val464Ala enzyme was also investigated at pH 6 where as illustrated in Figure S2 (Supporting Information), it was reduced to the hydroquinone state in a biphasic pattern, with a fast phase accounting for approximately 45−50% of the total change in absorbance, as compared to the 60−70% at pH 10.

With both the Val464Ala and Val464Thr enzymes, the observed rates for the fast phase of flavin reduction defined a rectangular hyperbola when plotted as a function of the concentration of choline (Figures 2B and S1 (Supporting Information)), as expected for an enzymatic kinetic process that reaches saturation. In contrast, a plot of the observed rates for the slow phase of flavin reduction as a function of the concentration of substrate yielded an inverse hyperbolic dependency, with the observed rates decreasing to an asymptotic value with increasing concentration of choline

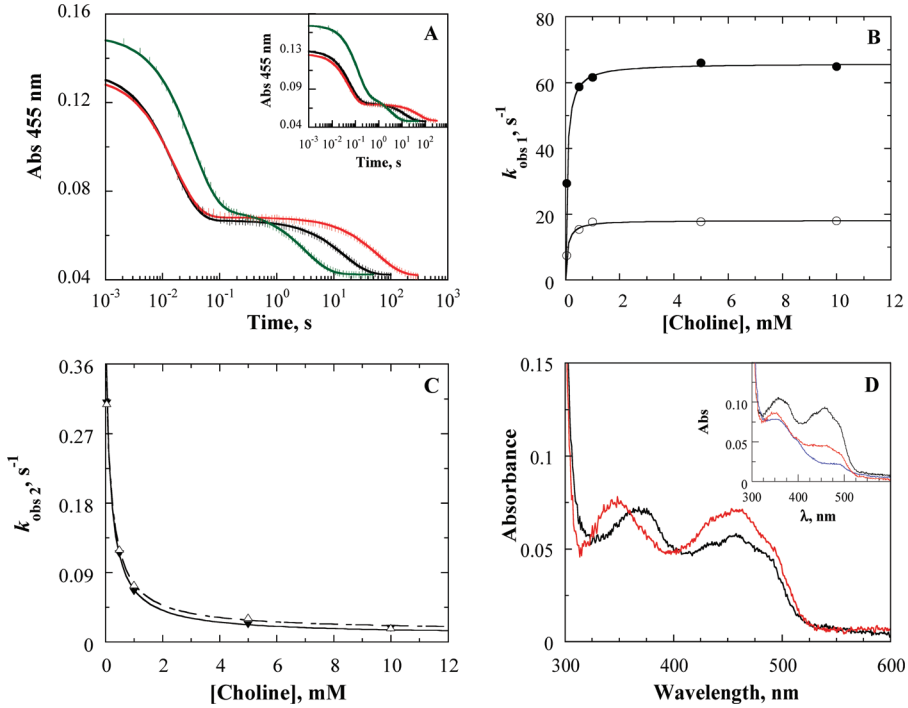

FIGURE 2: Anaerobic reduction of the Val464Thr enzyme with choline in 50 mM sodium pyrophosphate at pH 10 and 25 °C, monitored at 455 nm in a stopped-flow spectrophotometer. Panel A shows the reduction traces with 10 mM (red), 1 mM (black), and 0.05 mM (green) choline. Inset: reduction traces for the Val464Thr enzyme with 10 mM (red), 1 mM (black), and 0.05 mM (green) 1,2-[$^2H_4$]-choline. All traces were fit with eq 2. Time indicated is after the end of flow, i.e., 2.2 ms. For clarity, one experimental point out of every ten is shown (vertical lines). Panel B shows the observed rates as a function of substrate concentration for the fast phase of flavin reduction with choline (●) and 1,2-[$^2H_4$]-choline (○) as substrates. The curves are fits of the data with eq 3. Panel C shows the observed rates as a function of substrate concentration for the slow phase of flavin reduction with choline (▼) and 1,2-[$^2H_4$]-choline (△) as substrates. The curves are fits of the data with eq 4, e.g., $y = (0.009[s] + 0.072)/([s] + 0.183)$ ($R^2 = 0.9997$) with choline as a substrate. Panel D shows the UV−visible absorbance spectra of the catalytically competent form (black) and of the incompetent form (red) of the Val464Thr enzyme in complex with choline at pH 10 and 25 °C. Inset: UV−visible absorbance spectra determined with a PDA detector during the anaerobic reduction of the enzyme with 1 mM choline at 2.2 ms (black), 0.1 s (red), and 300 s (blue) after mixing the enzyme and the substrate in a stopped-flow spectrophotometer.

(Figures 2C and S1 (Supporting Information)). These kinetic data are readily accounted for with the kinetic mechanism of Scheme 3, in which a catalytically competent and active form of the enzyme (E_{ox}) is in slow equilibrium with a catalytically incompetent[2] species of enzyme (E^*_{ox}). Upon forming a Michaelis complex with the substrate, the competent $E^*_{ox}S$ species will continue through catalysis yielding reduced flavin and betaine aldehyde. In contrast, the incompetent $E^*_{ox}S$ species will either slowly re-equilibrate through its free form devoid of bound substrate with the E_{ox} form or directly convert to the competent $E_{ox}S$ complex, which will subsequently proceed through catalysis. Since substrate binding to the enzyme is a rapid equilibrium process, the rate of re-equilibration of the two forms of choline oxidase is limited by the conformational change involving both the free and enzyme−substrate complexes of the competent and incompetent forms of enzyme (defined by k_1, k_2, k_3, and k_4 in Scheme 3). According to this kinetic mechanism, the fast phase of flavin reduction seen in the stopped-flow traces represents the reduction of the $E_{ox}S$ species (k_{red} in Scheme 3), whereas the subsequent slow phase is due to the rate-limiting conformational change involving the two forms of enzyme. Fitting of the kinetic data[3] associated with the fast phase of flavin reduction to eq 3 allows for the determination of the first-order rate constant for flavin reduction (k_{red}), and the dissociation constant for the catalytically competent enzyme−substrate Michaelis complex (K_d). Fitting of the kinetic data associated with the slow phase of flavin reduction to eq 4 allows for the determination of the first-order rate constants for the conversion of the incompetent form of enzyme to the competent form of enzyme (k_1 and k_3) and of the dissociation constant for the catalytically incompetent enzyme−substrate complex (K_d*). Unfortunately, the requirement for pseudo-first-order conditions in the anaerobic reduction of the enzyme with choline did not allow for

[2] One of the two conformations of choline oxidase in which Val464 is replaced with alanine or threonine is defined in this study as incompetent, rather than inactive. The choice of the term stems from the kinetic mechanism of Scheme 3, which is the minimal mechanism that explains the experimental observations. Here, one species of enzyme is capable of oxidizing choline with a rate of hydride transfer that is not significantly different from that determined previously for the wild-type enzyme (i.e., ≥50.5 s^{-1} for Val464 variants; 93 s^{-1} for wild-type (*47*)). This form of enzyme is defined here as either competent or active. The other form of enzyme present in solution in the Val464 variants is either not capable of oxidizing the substrate or it oxidizes choline at a rate that is significantly lower than the rates governing the re-equilibration of the two forms of enzyme. Since the two possibilities cannot be discerned, we opted to define this form of enzyme as incompetent rather than inactive.

[3] The rationale for fitting the two phases seen in the reductive half-reaction catalyzed by the Val464Ala and Val464Thr enzymes with eqs 3 and 4 is that with both enzymes the fast phase is more than 5000-fold faster at saturating concentration of substrate than the slow phase of flavin reduction (Table 1). This implies an accumulation of an enzyme form (i.e., E^*_{ox} and $E^*_{ox}S$) in the kinetic pathway at the end of the fast phase of reduction, allowing for the kinetic treatment of the two phases as being independent from one another (*66*).

Table 1: Reductive Half-Reaction of the Val464Thr, Val464Ala and Wild-Type Enzymes with Choline as Substrate[a]

enzyme	k_{red} (s^{-1})	K_d (μM)	k_1 (s^{-1})	k_2 (s^{-1})	k_3 (s^{-1})	k_4 (s^{-1})	K_d* (μM)
Val464Ala	50.5 ± 2.4	≤50[b]	0.4 ± 0.01[b]	nd[c]	0.013 ± 0.001	nd[c]	≤80[b]
Val464Thr	65.8 ± 0.4	≤60[b]	0.4 ± 0.02[b]	nd[c]	0.009 ± 0.002	nd[c]	180 ± 10
Wild type (*47*)	93.1 ± 0.8	290 ± 10	no[d]	no[d]	no[d]	no[d]	no[d]

[a] Conditions: 50 mM sodium pyrophosphate, 25 °C, pH 10. [b] Better determinations could not be obtained due to the requirement of maintaining pseudo-first-order conditions in which the [substrate] was ≥5-times the [enzyme]. [c] nd, not determined. [d] no, not observed.

Table 2: Effect of Deuterated Substrate and Solvent on the Reductive Half-Reaction of the Val464Ala, Val464Thr, and Wild-Type Enzymes[a]

parameter	substrate	solvent	Val464Ala	Val464Thr	wild-type (*47*)
k_{red} (s^{-1})	choline	H_2O	50.5 ± 2.4	65.8 ± 0.4	93.1 ± 0.8
k_{red} (s^{-1})	choline	D_2O	12.0 ± 0.7	11.8 ± 0.3	94.0 ± 1.5
k_{red} (s^{-1})	1,2-[$^2H_4$]-choline	H_2O	17.2 ± 0.7	18.2 ± 0.3	10.3 ± 0.3
k_{red} (s^{-1})	1,2-[$^2H_4$]-choline	D_2O	13.2 ± 0.6	14.5 ± 0.1	10.9 ± 0.3
k_3 (s^{-1})	choline	H_2O	0.013 ± 0.001	0.009 ± 0.002	no[b]
k_3 (s^{-1})	choline	D_2O	0.004 ± 0.001	0.005 ± 0.001	no[b]
k_3 (s^{-1})	1,2-[$^2H_4$]-choline	H_2O	0.013 ± 0.001	0.010 ± 0.002	no[b]
k_3 (s^{-1})	1,2-[$^2H_4$]-choline	D_2O	0.006 ± 0.001	0.005 ± 0.001	no[b]

[a] Conditions: 50 mM sodium pyrophosphate, 25 °C, pH 10. Presteady-state kinetic parameters were determined by fitting the kinetic data acquired upon mixing anaerobically the enzyme with the substrate to eqs 3 and 4. All fits of the data yielded $R^2 \geq 0.99$. [b] no, not observed.

concentrations of choline below 50 μM to be used, thereby preventing an accurate determination of the first-order rate constant for the conversion of the E^*_{ox} form of choline oxidase to the E_{ox} species (k_1). All the relevant kinetic parameters determined in the reductive half-reactions with choline as substrate for the choline oxidase variants containing alanine or threonine at position 464 as well as the previously determined values for the wild-type enzyme (*47*) are summarized in Table 1.

The reductive half-reaction of the Val464Ala and Val464Thr enzymes with choline was also investigated with a PDA detector in order to gain insights on the UV−visible absorbance spectra of the enzyme−substrate complex species participating in the reaction. Relevant absorbance spectra of the species present right after anaerobic mixing of the enzyme and choline (2.2 ms), at the end of the fast phase of flavin reduction, and at the end of the slow phase of flavin reduction were collected. According to the mechanism of Scheme 3, only the fully reduced form of enzyme is present at the end of the reaction after both kinetic phases are completed. A mixture of fully reduced enzyme and incompetent enzyme−substrate complex populates the solution at the end of the fast phase of flavin reduction. Finally, a mixture of incompetent and competent enzyme−substrate complexes is present right after anaerobic mixing of the enzyme with choline. The relative amounts of competent and incompetent forms of the enzymes could be estimated from the amplitudes of the kinetic phases observed in the stopped-flow traces, allowing the extraction of the UV−visible absorbance spectra for the competent and incompetent forms of the Val464 variants of choline oxidase in complex with the substrate (e.g., The UV−visible absorbance spectrum for $E^*_{ox}S$ can be extracted by taking the spectrum at the end of the fast phase (red trace in Figure 2D inset) and subtracting the quota of the fully reduced spectrum (blue trace in Figure 2D inset) corresponding to the relative amount of E_{ox}. Subtraction of the extracted spectrum for $E^*_{ox}S$ from the initial spectrum (black trace in Figure 2D inset) will in turn yield the $E_{ox}S$ spectrum). As shown in Figures 2D and S1 (Supporting Information), a significant hypsochromic shift of at least 20 nm is observed in the high energy absorbance band of the incompetent enzyme−substrate complexes as compared to their competent counterparts for both the Val464Ala and Val464Thr enzymes.

Substrate Deuterium Kinetic Isotope Effects. Substrate kinetic isotope effects were employed with the dual goal of assessing the validity of the kinetic mechanism of Scheme 3 and gaining insights into the status of the CH bond of choline in the transition state for the reactions catalyzed by the Val464Ala and Val464Thr enzymes. As shown in Figures 2B and S1 (Supporting Information), a significant decrease in the observed rates for the fast phase of flavin reduction was seen upon substituting choline with 1,2-[$^2H_4$]-choline in H_2O, suggesting that the reaction of flavin reduction, which is concomitant to the cleavage of the CH bond of choline, is at least partially rate-limiting for the reductive half-reaction in H_2O. However, when the flavin reduction was performed in D_2O the $^D(k_{red})_{D_2O}$ values for both investigated enzymes were not significantly different from unity as compared to $^D(k_{red})_{H_2O}$ values ≥2.9, indicating that the cleavage of the substrate CH bond in deuterium oxide is not rate-limiting for the overall reductive half-reaction. In contrast, there was no difference in the observed rates for the slow phase of flavin reduction when choline was substituted with 1,2-[$^2H_4$]-choline for both enzymes (Figures 2C and S1 (Supporting Information)) irrespective of the isotopic composition of the solvent. These kinetic data further support the kinetic mechanism of Scheme 3, for which a significant substrate kinetic isotope effect is predicted for the fast phase of flavin reduction, whereas no substrate isotope effect is expected for the conformational change occurring between the competent and incompetent enzyme species. Tables 2 and 3 summarize the kinetic parameters and the related kinetic isotope effects for the reductive half-reactions of the Val464Ala, Val464Thr, and the wild-type (*47*) enzymes determined with choline and 1,2-[$^2H_4$]-choline as substrate.

Solvent Deuterium Kinetic Isotope Effects. Solvent deuterium kinetic isotope effects were used to probe the status of the OH bond of choline in the transition state for the reaction of hydride transfer catalyzed by the variants of choline oxidase substituted at position 464. The anaerobic flavin reduction reaction was investigated in H_2O and D_2O, and the relevant $^{D_2O}(k_{red})$ and $^{D_2O}(k_3)$ values were determined at pL 10 and 25 °C with either choline or 1,2-[$^2H_4$]-choline.

Table 3: Substrate and Solvent Deuterium Kinetic Isotope Effects on the Reductive Half-Reaction of the Val464Ala, Val464Thr, and Wild-Type Enzymes[a]

parameter	Val464Ala	Val464Thr	wild-type (*47*)
$^{D}(k_{red})_{H_2O}$	2.9 ± 0.1	3.6 ± 0.1	8.9 ± 0.2
$^{D}(k_{red})_{D_2O}$	0.9 ± 0.1	0.8 ± 0.1	8.7 ± 0.2
$^{D_2O}(k_{red})_{H}$	4.2 ± 0.4	5.6 ± 0.1	0.99 ± 0.1
$^{D_2O}(k_{red})_{D}$	1.3 ± 0.1	1.3 ± 0.1	0.94 ± 0.1
$^{D}(k_3)_{H_2O}$	1.0 ± 0.1	0.9 ± 0.1	no[b]
$^{D}(k_3)_{D_2O}$	0.8 ± 0.2	1.1 ± 0.3	no[b]
$^{D_2O}(k_3)_{H}$	3.0 ± 0.4	1.7 ± 0.4	no[b]
$^{D_2O}(k_3)_{D}$	2.3 ± 0.4	2.1 ± 0.3	no[b]

[a] Conditions: 50 mM sodium pyrophosphate, 25 °C, pL 10. [b] no, not observed.

Table 4: Effect of Glucose and PEG-6000 on the Reductive Half-Reaction of the Val464Thr Enzyme with Choline as Substrate[a]

parameter	viscosigen[b]	Val464Thr
$(k_{red})_{glucose}$ (s^{-1})	glucose	48.1 ± 0.3
$(k_{red})_{PEG}$ (s^{-1})	PEG	48.1 ± 1.6
$(k_3)_{glucose}$ (s^{-1})	glucose	0.010 ± 0.003
$(k_3)_{PEG}$ (s^{-1})	PEG	0.019 ± 0.003
$k_{red}/(k_{red})_{glucose}$		1.36 ± 0.02
$k_{red}/(k_{red})_{PEG}$		1.37 ± 0.05
$k_3/(k_3)_{glucose}$		0.9 ± 0.3
$k_3/(k_3)_{PEG}$		0.5 ± 0.3

[a] Conditions: 50 mM sodium pyrophosphate, 25 °C, pH 10. [b] Solvent contained 8% glucose, equivalent to a relative viscosity of 1.25 (*58*), or 0.0211 g/mL of PEG-6000, equivalent to a relative viscosity of 1.26 (*59*).

As expected, both the Val464Ala and Val464Thr enzymes showed $^{D_2O}(k_{red})_{H}$ values of at least 4 with choline as substrate, consistent with these effects directly reporting on the status of the OH bond in the transition state for the reaction catalyzed by the enzymes. When 1,2-[$^2H_4$]-choline was used instead of choline, a significant decrease in the $^{D_2O}(k_{red})_{D}$ to a value of 1.3 was observed with both enzymes (Table 3), suggesting that slowing down the cleavage of the CH bond of the substrate masks the solvent kinetic isotope effects. The $^{D_2O}(k_3)$ values were significantly larger than unity irrespective of whether choline or 1,2-[$^2H_4$]-choline was used as substrate for the Val464 enzyme variants (Table 3), consistent with the re-equilibration of the competent and incompetent forms of enzyme being sensitive to the isotopic composition of the solvent.

Solvent Viscosity Effects. The effect of solvent viscosity on the reductive half-reaction of the Val464Thr enzyme was investigated to establish whether the observed solvent kinetic isotope effects are associated with the cleavage of the OH bond of choline or simply due to the increased viscosity of D_2O with respect to H_2O. The reductive half-reaction of the Val464Thr enzyme with choline was consequently investigated at pH 10 and 25 °C in solutions containing 8% glucose or 0.0211 g/mL PEG-6000, which provide solvent viscosities equivalent to a 100% solution of D_2O. As illustrated in the data of Table 4, similar k_{red} values, which were smaller than those seen in a control experiment in the absence of viscosigens, were determined in the presence of glucose and PEG-6000, suggesting that no effect other than solvent viscosity was present on the kinetic step of flavin reduction. As summarized in Table 4, solvent viscosity effects on the k_{red} values of 1.4 were observed with choline as substrate, which were significantly larger than unity and lower than the $^{D_2O}(k_{red})_{H}$ values of ≥4, suggesting that solvent viscosity plays a significant, but not prominent, role in the kinetic step

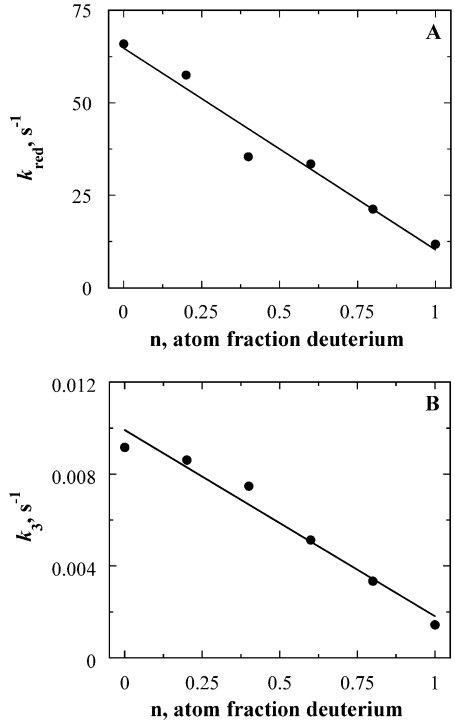

FIGURE 3: Rates of anaerobic flavin reduction measured in a stopped-flow spectrophotometer as a function of the mole fraction (n) of deuterium oxide associated with the fast (k_{red}) and slow (k_3) phases of reduction for Val464Thr. Panel A is the proton inventory of the k_{red} value. Panel B is the proton inventory of the k_3 value. The lines represent linear fits of the data.

of cleavage of the substrate OH bond in the reaction catalyzed by the Val464Thr enzyme. In contrast, slightly inverse (i.e., ≤1) effects were seen on the k_3 values in the presence of glucose or PEG-6000 (Table 4). These data suggest that the normal (i.e., ≥1) effects observed on the $^{D_2O}(k_3)$ values primarily originate from solvent sensitive steps that directly involve proton abstraction from OH group(s).

Proton Inventories. The reductive half-reaction of the Val464Ala and Val464Thr enzymes was investigated in solutions with varying mole fractions of deuterium oxide to gain insights into the number of exchangeable protons involved in the fast and slow phases of anaerobic flavin reduction. As shown in Figures 3A and S3 (Supporting Information), linear relationships were seen upon plotting the k_{red} values as a function of the mole fraction of deuterated solvent, suggesting that a single proton is in flight in the transition state for the reaction of flavin reduction catalyzed by the choline oxidase variants containing alanine or threonine at position 464. Similar linear relationships were observed with both enzymes in the proton inventories associated with the k_3 value (Figures 3B and S3 (Supporting Information)), also consistent with a single proton being in flight in the kinetic step involving the conformational change of the incompetent enzyme to the competent form of the enzyme.

Effect of pH on the UV−Visible Absorbance Spectra of Free Oxidized Variant Enzymes. The pH dependence of the UV−visible absorbance spectra of the variant enzymes was determined to establish whether the pK_a values for the 8α-*N*(3)-histidyl-FAD of choline oxidase were affected by replacing the valine at position 464 with alanine or threonine. As the pH is increased from 6 to ~10.4, a progressive decrease in the absorbance at ~380 nm, ~460 nm, and ~490 nm was observed (Figures 4A and S4 (Supporting Informa-

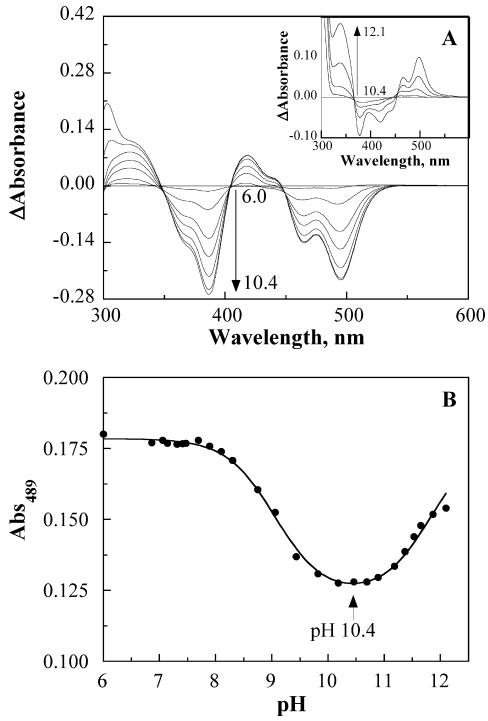

FIGURE 4: pH dependence of the UV−visible absorbance spectra of Val464Thr. Absorbance spectra at varying pH were recorded in 20 mM sodium phosphate and 20 mM sodium pyrophosphate, at 15 °C, starting at pH 6 and increasing the pH with addition of NaOH. Panel A shows the selected difference absorbance spectra (spectrum pH x – spectrum pH 6) in the pH range from 6 to 10.4. The inset shows selected difference absorbance spectra (spectrum pH x – spectrum pH 10.4) in the pH range from 10.4 to 12.1. Arrows indicate the direction of increasing pH. Panel B shows the dependence of the UV−visible absorbance values at 489 nm for the Val464Thr enzyme on pH; the data were fit with eq 5.

tion)). Further increase of the pH above 10.4 yielded an inversion of the spectral changes at the three wavelengths, as clearly shown in Figures 4B and S4 (Supporting Information) for the case of ~490 nm. The observed spectral changes, along with the fitting of the data with eq 5, are consistent with the presence of two pK_a values associated with the ionization of the histidyl residue linking the flavin to the polypeptide chain (i.e., His99), and the N(3) atom of the isoalloxazine ring of the flavin (*62*−*65*). The relevant pK_a values for the Val464Ala and Val464Thr enzymes are summarized in Table 5, along with the previously determined value for the wild-type form of choline oxidase[4].

Table 5: Comparison of the pK_a Values Associated with the Ionization of the Enzyme-Bound Oxidized Form of 8α-*N*(3)-Histidyl-FAD in the Val464Ala, Val464Thr, and His466Ala Enzymes with Wild-Type Choline Oxidase[a]

enzyme	His99	flavin N(3)
Val464Ala	9.1 ± 0.1	≥11.7
Val464Thr	9.1 ± 0.1	≥12
His466Ala[b]	9.3 ± 0.2	nd[c]
wild-type[b]	8.2 ± 0.1	nd[c]

[a] Conditions: 20 mM sodium pyrophosphate, 20 mM sodium phosphate, and 15 °C. [b] Data are from ref *49*. [c] nd, not determined.

DISCUSSION

In this study, the hydrophobic residue Val464 lining the top of the active site cavity in proximity to the N(5) atom of the flavin cofactor of choline oxidase was replaced with either threonine or alanine to establish its role in the reductive half-reaction in which a hydride ion is transferred from choline to the flavin. The resulting Val464Thr and Val464Ala enzyme variants are properly folded, stable, and functional, as suggested by a number of biophysical and biochemical properties that are in common with the wild-type form of choline oxidase. The Val464 variants contain FAD covalently linked to the protein moiety, stabilize an anionic flavosemiquinone at pH 8.0 in the presence of air, display UV−visible absorbance spectra with no sign of protein denaturation, have k_{red}, K_d, and $^Dk_{red}$ values that are within 3-fold from the values shown for the wild-type enzyme. Consequently, the role of the Val464 residue in the reaction of hydride transfer catalyzed by choline oxidase can be established by comparing and contrasting the kinetic and mechanistic properties of the enzyme variants containing threonine or alanine at position 464 with those of the wild-type enzyme containing valine.

The hydrophobic residue at position 464 is important for the proper assembly of the catalytic machinery required for the reaction of choline oxidation catalyzed by choline oxidase. Indeed, the most dramatic effect of replacing Val464 with either a threonine or alanine is the stabilization of a catalytically incompetent form of enzyme that reversibly, slowly equilibrates with a form of enzyme that can oxidize choline. The conformational change that interconverts the two forms of enzyme occurs on both the free species of choline oxidase devoid of ligands in the active site as well as the enzyme substrate complexes (Scheme 3) is associated with changes in the ionization state of a group on the enzyme, which is not readily available to the bulk solvent. This conclusion is supported by the results of proton inventory on the anaerobic reduction of the flavin with choline, showing a linear dependence of the mole fraction of deuterated solvent on the rate constant for the conversion of the incompetent form of choline oxidase to the active form (k_3). The spectroscopic properties of the Val464 variant enzymes in their catalytically incompetent and active forms further suggest that the ionizable group associated with the loss of catalytic activity must be linked to the flavin cofactor via a covalent bond, one or more hydrogen bonds, or electrostatic interactions. In this regard, upon replacing Val464 with threonine or alanine there is a one unit increase of the pK_a value for the ionization of the side chain of His99, which is the site of covalent attachment of the polypeptide to the C(8) methyl group of the flavin (*54*). This raises the attractive possibility that His99 may be involved in the formation and stabilization of the incompetent form of choline oxidase (see below). In support of this hypothesis is the 20 nm hypsochromic shift of the high energy band of FAD seen in the UV−visible absorbance spectra of the catalytically incompetent form of the Val464Ala and Val464Thr enzymes with respect to the active form, which is expected for a change in the ionization of an 8α-*N*(3)-histidyl-flavin (*63*−*65*).

[4] In the course of an independent study on a number of choline oxidase variants in which serine 101 and histidine 99 is replaced with other amino acid residues (Yuan, H., and Gadda, G., manuscript in preparation), we realized that our initial assignments of the pK_a values associated with the UV−visible absorbance spectra for the wild-type and the variant enzyme His466Ala of choline oxidase published in ref *49* are incorrect. In that study, we erroneously assigned the pK_a values observed at 8.2 and 9.3 to the N(3) atom of the flavin, rather than the histidyl residue covalently linking the flavin to the polypeptide chain (His99).

Further evidence of a change in ionization being involved in the inactivation of the enzyme is observed in the difference in the relative amounts of active and inactive forms of the investigated Val464 variant enzymes at pH 6 and 10.

Replacement of Val464 with threonine or alanine significantly slows down the cleavage of the OH bond of choline in the oxidation reaction catalyzed by choline oxidase. In this regard, in the wild-type enzyme it was previously shown that the cleavage of the OH bond is considerably faster than the cleavage of the CH bond of choline, as indicated by $^{D_2O}(k_{red})_H$ values of 0.99 and $^{D}(k_{red})_{H_2O}$ values of 8.9 (*47*). In contrast, in the reactions catalyzed by the Val464Ala and Val464Thr enzymes the abstraction of the hydroxyl proton and the cleavage of the CH bond are both associated with deuterium kinetic isotope effects significantly larger than unity, with $^{D_2O}(k_{red})_H$ values $\geq$4.2 and $^{D}(k_{red})_{H_2O}$ values between 2.9 and 3.6. Interestingly, both cleavages of the OH and CH bonds contribute to different extents to the overall rate of flavin reduction depending upon the isotopic composition of the solvent or the substrate, consistent with the two steps having rate constants of similar magnitude. The similar increases of the pK_a values for the 8-α-*N*(3)-histidyl-flavin seen upon replacing Val464 with threonine or alanine and His466 with alanine (*49*) suggest that the slower rate of hydroxyl proton abstraction in the valine substituted enzymes may be due to a different positioning of His466, the flavin N(5) atom, or both with respect to the initial alcohol substrate, as His466 was previously shown to facilitate hydroxyl proton abstraction by stabilizing the alkoxide species in catalysis (*49*).

Substitution of Val464 with alanine or threonine has a minimal effect on the rate of hydride ion transfer from the α-carbon of the alkoxide species formed in catalysis and the N(5) atom of the flavin cofactor. Evidence supporting this conclusion comes from the comparison of the k_{red} values with 1,2-[$^2H_4$]-choline, which primarily reflect the cleavage of the substrate CH bond, for the Val464Ala or Val464Thr enzymes with earlier data obtained with the wild-type enzyme, showing comparable rate constants (i.e., ~17 s^{-1} for the Val464 variants, as compared to 10.4 s^{-1} for the wild-type enzyme (*47*)).

The abstraction of the hydroxyl proton of choline in the enzyme variants substituted on Val464 is associated with an isomerization of the enzyme−substrate complex, as suggested by the effects of solvent viscosity on the rate constant for flavin reduction decreasing by ~40% in the presence of viscosigens. Since a reaction of hydroxyl proton abstraction per se is not expected to depend on the viscosity of the solvent, the effect of solvent viscosity must arise from a solvent sensitive internal equilibrium between a choline−enzyme complex and a choline alkoxide−protonated enzyme complex. An internal equilibrium of the enzyme−substrate complex was proposed earlier for the wild-type form of choline oxidase based on the enthalpy of activation ($\Delta H^{\ddagger}$) for the reaction of hydride ion transfer under reversible catalytic regime being significantly larger than the $\Delta H^{\ddagger}$ value for the reaction under irreversible catalytic regime (*53*). In that case, it was demonstrated that the environmental organization required in the enzyme−substrate complex to bring the hydride donor and acceptor in a preorganized configuration suitable for environmentally assisted tunneling is linked to the conformational change associated with the hydroxyl proton abstraction (*48, 53*). Furthermore, both solvent viscosity and substrate kinetic isotope effects on the steady state kinetic parameters for the reaction of a choline oxidase variant in which Glu312 is substituted with aspartate were also interpreted with the presence of an internal equilibrium of the enzyme−substrate complex preceding the hydride transfer reaction (*54*).

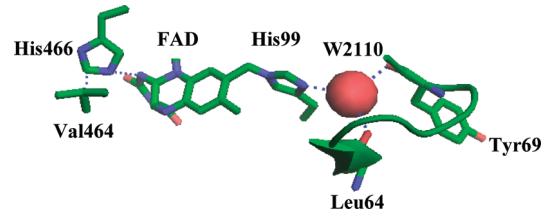

FIGURE 5: Close-up view of the active site of the wild-type form of choline oxidase showing the hydrogen bonding interactions involving the N(1) atom of His99, a structural water molecule (W2110) secluded from the bulk solvent, the peptidyl oxygen atoms of Leu64 and Tyr69, the van der Waals interaction between a methyl group of Val464 and the C(2) atom of His466, and the hydrogen bonding interaction of the N(3) atom of His466 and the N(1) atom of the flavin cofactor (PDB entry 2jbv).

The structural information on the wild-type form of choline oxidase provides a solid framework to substantiate the hypothesis of an involvement of His99 in the inactivation of the enzyme. Indeed, the N(1) atom of His99 is located in a small cavity that is completely secluded from the bulk solvent, in hydrogen bonding distance (2.9 Å) with a structural water molecule (W2110). This water molecule, in turn, is in hydrogen bonding distance with the peptidyl oxygen atoms of Leu64 (3.1 Å) and Tyr69 (3.0 Å) located on a long loop (residues 64−95) covering the active site of the enzyme (Figure 5) (*54*). A change in the ionization state of His99 is expected to affect the hydrogen bonding pattern around W2110, conceivably resulting in a change in the conformation of the enzyme. The link between Val464 and His99, which are spatially located 10.6 Å away from one another, is likely provided by His466. Since the C(2) atom of His466 is in van der Waals contact with a methyl group of Val464 (3.2 Å) and its N(3) atom is in hydrogen bonding distance from the N(1) atom of the flavin (3.2 Å) (Figure 5), it is expected that substitution of the hydrophobic side chain at position 464 (Val) with a hydrophilic side chain (Thr) or with an amino acid with a shorter side chain (Ala) would affect the interaction of His466 with the flavin isoalloxazine moiety. In support of this conclusion is the observation that both the replacements of Val464 with threonine or alanine and of His466 with alanine have the same effect of increasing the pK_a value for the ionization of the N(1) atom of His99 from 8.2 to ~9.1 (*49*).

In conclusion, the results presented in this study on the enzyme variants of choline oxidase in which Val464 has been replaced with alanine or threonine allow us to conclude that the hydrophobic residue Val464 lining the active site cavity close to the N(5) atom of the flavin, although not directly participating in catalysis, is important for the positioning of the catalytic groups in the active site of the enzyme. Replacement of Val464 with alanine or threonine has uncovered a kinetically slow equilibrium between a catalytically incompetent form of enzyme and a form of enzyme that maintains the ability to efficiently oxidize the alcohol substrate. From a mechanistic standpoint, a major effect of the presence of a hydrophilic residue at position 464 is to considerably decrease

the rate of hydroxyl proton abstraction from the substrate in the reaction of choline oxidation, with a minimal effect on the rate of hydride ion transfer from the alkoxide species to the N(5) flavin atom. The replacement of Val464 with threonine or alanine is likely to affect the preorganization of the enzyme−substrate complex that undergoes the hydride transfer reaction. In this respect, it will be of interest to tailor future studies toward addressing to which extent a mutation of a residue not directly participating in catalysis, such as Val464, may affect the mode of hydride ion transfer.

ACKNOWLEDGMENT

We thank Andrea Pennati, Hongling Yuan, Kevin Francis, Osbourne Quaye, and Kunchala Rungsrisuriyachai for helpful discussions. We also thank Kevin Francis for the critical reading of the manuscript.

APPENDIX

The proposed mechanism for the reaction catalyzed by the choline oxidase variants Val464Ala and Val464Thr in which both the free enzymes and enzyme−substrate complexes can interconvert (*61*) is described. The derivation of the equation that describes the rate of the second phase of flavin reduction follows the logic described by Frederick and Palfey (*61*) and the method laid forth by Cha (*60*).

Scheme A1

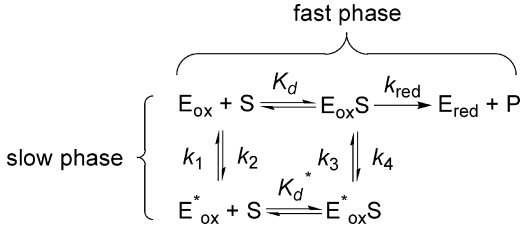

ASSUMPTIONS

Free E_{ox} and E^*_{ox} binding with substrate is in rapid equilibrium. This allows for the simplification of Scheme A1 to yield a partial equilibrium mechanism shown in Scheme A2.

Scheme A2

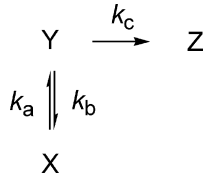

In Scheme A2, X represents the rapid equilibrium segment for E^*_{ox} binding to substrate, Y represents the rapid equilibrium segment for E_{ox} binding to substrate, and Z is the reduced enzyme and product. The rate constants k_a and k_b are apparent rate constants that represent the rate of interconversion of the two rapid equilibrium segments, and k_c is the apparent rate of flavin reduction.

$$k_a = k_3 f_{E^*_{ox}S} + k_1 f_{E^*_{ox}} \tag{A1}$$

$$k_b = k_4 f_{E_{ox}S} + k_2 f_{E_{ox}} \tag{A2}$$

$$k_c = k_{red} f_{E_{ox}S} \tag{A3}$$

Where $f_{E^*_{ox}S}$, $f_{E^*_{ox}}$, $f_{E_{ox}S}$, and $f_{E_{ox}}$ are fractional concentration factors defining the fraction of the total enzyme within a rapid equilibrium segment of a given enzyme species.

$$f_{E^*_{ox}S} = \frac{[s]}{[s] + K^*_d} \tag{A4}$$

$$f_{E^*_{ox}} = \frac{K^*_d}{[s] + K^*_d} \tag{A5}$$

$$f_{E_{ox}S} = \frac{[s]}{[s] + K_d} \tag{A6}$$

$$f_{E_{ox}} = \frac{K_d}{[s] + K_d} \tag{A7}$$

The change of the relative amounts of enzyme in a given rapid equilibrium segment can be described by the following differential equations:

$$\frac{dX}{dt} = -k_a X + k_b Y \tag{A8}$$

$$\frac{dY}{dt} = k_a X - (k_b + k_c) Y \tag{A9}$$

$$\frac{dZ}{dt} = k_c Y \tag{A10}$$

The fast reaction is ~5000 times faster when the substrate is saturating ($[s] >> K_d$ and K^*_d) than the slow reaction, meaning that the initial amount of *Y*, Y_0 has reacted completely before any significant fraction of incompetent enzyme is converted to the competent form. This means that upon onset of the second phase, the initial amount of *X*, X_0 will either still be in the form of *X* or will have converted to *Y* or *Z*.

$$X_0 = X + Y + Z \leftrightarrow X = X_0 - Y - Z \tag{A11}$$

Assuming steady state for Y

$$\frac{dY}{dt} = k_a X - (k_a + k_c) \mathrm{Y} = 0 \tag{A12}$$

Insert the above expression for X (eq A11) into the differential equation for Y (eq A12).

$$0 = k_a(X_0 - Y - Z) - (k_b + k_c) Y \leftrightarrow$$

$$Y = \frac{k_a(X_0 - Z)}{(k_a + k_b + k_c)} \tag{A13}$$

Insert expression for *Y* (eq A13) into the differential equation for *Z* (eq A10) and solve for *Z*.

$$\frac{dZ}{dt} = k_c Y = k_c \frac{k_a(X_0 - Z)}{(k_a + k_b + k_c)} =$$

$$\frac{k_c k_a X_0}{(k_a + k_b + k_c)} - \frac{k_c k_a}{(k_a + k_b + k_c)} Z =$$

$$kX_0 - kZ = k(X_0 - Z) \leftrightarrow$$

$$\frac{dZ}{X_0 - Z} = kdt \leftrightarrow \int \frac{dZ}{X_0 - Z} = \int kdt \leftrightarrow$$

$$-\ln(X_0 - Z) = kt + c, t = 0 \Rightarrow Z = 0 \leftrightarrow$$

$$Z = X_0 - X_0 \, e^{kt}, k = \frac{k_c k_a}{(k_a + k_b + k_c)} \tag{A14}$$

Insert the expressions for k_a, k_b, and k_c (eqs A1−A3) into the term for the observed rate (eq A14):

$$k_{obs_2} = \frac{k_d k_c}{k_a + k_b + k_c} \leftrightarrow$$

$$k_{obs_2} = \frac{\dfrac{k_3[s] + k_1 K_d^*}{K_d^* + [s]} \cdot \dfrac{k_{red}[s]}{K_d + [s]}}{\dfrac{k_3[s] + k_1 K_d^*}{K_d^* + [s]} + \dfrac{k_2 K_d + k_4[s]}{K_d + [s]} + \dfrac{k_{red}[s]}{K_d + [s]}} \leftrightarrow$$

$$k_{obs_2} = \frac{(k_3[s] + k_1 K_d^*)(k_{red}[s])}{(k_3[s] + k_1 K_d^*)(K_d + [s]) + (k_2 K_d + k_4[s])(K_d^* + [s]) + k_{red}[s](K_d^* + [s])} \leftrightarrow$$

$$k_{obs_2} = \frac{k_{red} k_3[s]^2 + k_{red} k_1 K_d^*[s]}{(k_3 + k_4 + k_{red})[s]^2 + ((k_3 + k_2)K_d + (k_1 + k_4 + k_{red})K_d^*)[s] + (k_1 + k_2)K_d K_d^*}$$

$k_{red} >> k_1$, k_2, k_3, k_4 allowing to reduce the equation to:

$$k_{obs_2} = \frac{k_{red} k_3[s]^2 + k_{red} k_1 K_d^*[s]}{k_{red}[s]^2 + ((k_3 + k_2)K_d + (k_{red})K_d^*)[s] + (k_1 + k_2)K_d K_d^*}$$

At [S] $>>$ K_d and K_d^*, allowing to reduce the equation to:

$$k_{obs_2} = \frac{k_{red} k_3[s]^2 + k_{red} k_1 K_d^*[s]}{k_{red}[s]^2 + ((k_3 + k_2)K_d + (k_{red})K_d^*)[s]}$$

set $K_d = \alpha K_d^*$

$$k_{obs_2} = \frac{k_{red} k_3[s]^2 + k_{red} k_1 K_d^*[s]}{k_{red}[s]^2 + ((k_3 + k_2)\alpha K_d^* + (k_{red})K_d^*)[s]} \leftrightarrow$$

$$k_{obs_2} = \frac{k_{red} k_3[s]^2 + k_{red} k_1 K_d^*[s]}{(k_{red})[s]^2 + ((\alpha k_3 + \alpha k_2 + k_{red})K_d^*)[s]} \leftrightarrow$$

$$k_{obs_2} = \frac{k_{red} k_3[s]^2 + k_{red} k_1 K_d^*[s]}{k_{red}[s]^2 + (k_{red} K_d^*)[s]} = \frac{k_3[s] + k_1 K_d^*}{[s] + K_d^*} \quad \text{(A15)}$$

The limiting values for the observed rate of flavin reduction:

$$\lim_{[s]\to\infty} k_{obs_2} = k_3 \quad \text{(A16)}$$

$$\lim_{[s]\to 0} k_{obs_2} = k_1 \quad \text{(A17)}$$

SUPPORTING INFORMATION AVAILABLE

Figure S1 shows the anaerobic reduction of the Val464Ala enzyme at pH 10; Figure S2 shows the anaerobic reduction of the Val464Ala enzyme at pH 6; Figure S3 shows the rates of flavin reduction as a function of the mole fraction of deuterium oxide for Val464Ala; Figure S4 shows pH dependence of the UV−visible absorbance spectra of Val464Ala. This material is available free of charge via the Internet at http://pubs.acs.org.

REFERENCES

1. Csonka, L. N., and Epstein, W. (1996) Osmoregulation, in *Escherichia coli and Salmonella: Cellular and Molecular Biology* (Neidhardt, F. C., Curtis, R., III, Ingraham, J. L., Lin, E. C. C., Low, K. B., Magasanik, B., Reznikoff, W. S., Riley, M., Schaechter, M., and Umbarger, H. E., Eds.) pp 1210−1223, ASM Press, Washington, D.C.
2. Burg, M. B., Kwon, E. D., and Kultz, D. (1997) Regulation of gene expression by hypertonicity. *Annu. Rev. Physiol. 59*, 437–455.
3. Kempf, B., and Bremer, E. (1998) Uptake and synthesis of compatible solutes as microbial stress responses to high-osmolality environments. *Arch. Microbiol. 170*, 319–330.
4. McNeil, S. D., Nuccio, M. L., and Hanson, A. D. (1999) Betaines and related osmoprotectants. Targets for metabolic engineering of stress resistance. *Plant Physiol. 120*, 945–950.
5. Bremer, E., andKramer, R. (2000) Coping with Osmotic Challanges: Osmoregulation through Accumulation and Release of Compatible Solutes in Bacteria, in *Bacterial Stress Response* (Storz, G., and Hengge-Areonis, R., Eds.), pp 79−97, ASM Press, Washington, D.C.
6. Sakamoto, A., Alia, Murata, N., and Murata, A. (1998) Metabolic engineering of rice leading to biosynthesis of glycinebetaine and tolerance to salt and cold. *Plant Mol. Biol. 38*, 1011–1019.
7. Waditee, R., Bhuiyan, N. H., Hirata, E., Hibino, T., Tanaka, Y., Shikata, M., and Takabe, T. (2007) Metabolic engineering for betaine accumulation in microbes and plants. *J. Biol. Chem. 282*, 34185–34193.
8. Quan, R., Shang, M., Zhang, H., Zhao, Y., and Zhang, J. (2004) Engineering of enhanced glycine betaine synthesis improves drought tolerance in maize. *J. Plant Biotechnol. 2*, 477–486.
9. Sakamoto, A., Valverde, R., Alia, Chen, T. H., and Murata, N. (2000) Transformation of *Arabidopsis* with the *codA* gene for choline oxidase enhances freezing tolerance of plants. *J. Plant. 22*, 449–453.
10. Alia, K. Y., Sakamoto, A., Nonaka, H., Hayashi, H., Saradhi, P. P., Chen, T. H., and Murata, N. (1999) Enhanced tolerance to light stress of transgenic *Arabidopsis* plants that express the *codA* gene for a bacterial choline oxidase. *Plant. Mol. Biol. 40*, 279–288.
11. Holmstrom, K. O., Somersalo, S., Mandal, A., Palva, T. E., and Welin, B. (2000) Improved tolerance to salinity and low temperature in transgenic tobacco producing glycine betaine. *J. Exp. Bot. 51*, 177–185.
12. Deshnium, P., Gombos, Z., Nishiyama, Y., and Murata, N. (1997) The action in vivo of glycine betaine in enhancement of tolerance of *Synechococcus* sp. strain PCC 7942 to low temperature. *J. Bacteriol. 179*, 339–344.
13. Deshnium, P., Los, D. A., Hayashi, H., Mustardy, L., and Murata, N. (1995) Transformation of *Synechococcus* with a gene for choline oxidase enhances tolerance to salt stress. *Plan. Mol. Biol. 29*, 897–907.
14. Lisa, T. A., Casale, C. H., and Domenech, C. E. (1994) Cholinesterase, acid phosphatase, and phospholipase C of *Pseudomonas aeruginosa* under hyperosmotic conditions in a high-phosphate medium. *Curr. Microbiol. 28*, 71–76.
15. Pesin, S. R., and Candia, O. A. (1982) Acetylcholine concentration and its role in ionic transport by the corneal epithelium. *Invest. Ophthalmol. Vis. Sci. 22*, 651–659.
16. Wright, J. R., and Clements, J. A. (1987) Metabolism and turnover of lung surfactant. *Am. Rev. Respir. Dis. 136*, 426–444.
17. Kilbourne, J. P. (1978) Bacterial content and ionic composiiton of sputum in cystic fibrosis. *Lancet* 334.
18. Peddie, B. A., Chambers, S. T., and Lever, M. (1996) Is the ability of urinary tract pathogens to accumulate glycine betaine a factor in the virulence of pathogenic strains? *J. Lab. Clin. Med. 128*, 417–422.
19. Culham, D. E., Emmerson, K. S., Lasby, B., Mamelak, D., Steer, B. A., Gyles, C. L., Villarejo, M., and Wood, J. M. (1994) Genes encoding osmoregulatory proline/glycine betaine transporters and the proline catabolic system are present and expressed in diverse clinical *Escherichia coli* isolates. *Can. J. Microbiol. 40*, 397–402.
20. Kunin, C. M., and Rudy, J. (1991) Effect of NaCl-induced osmotic stress on intracellular concentrations of glycine betaine and potassium in *Escherichia coli, Enterococcus faecalis*, and *staphylococci*. *J. Lab. Clin. Med. 118*, 217–224.
21. Landfald, B., and Strom, A. R. (1986) Choline-glycine betaine pathway confers a high level of osmotic tolerance in *Escherichia coli*. *J. Bacteriol. 165*, 849–855.
22. Lucht, J. M., and Bremer, E. (1994) Adaptation of *Escherichia coli* to high osmolarity environments: osmoregulation of the high-affinity glycine betaine transport system *proU*. *FEMS Microbiol. Rev. 14*, 3–20.

23. Badger, J. L., and Kim, K. S. (1998) Environmental growth conditions influence the ability of *Escherichia coli* K1 to invade brain microvascular endothelial cells and confer serum resistance. *Infect. Immun. 66*, 5692–5697.
24. Schwan, W. R., Lee, J. L., Lenard, F. A., Matthews, B. T., and Beck, M. T. (2002) Osmolarity and pH growth conditions regulate *fim* gene transcription and type 1 pilus expression in uropathogenic *Escherichia coli*. *Infect. Immun. 70*, 1391–1402.
25. Rachid, S., Ohlsen, K., Witte, W., Hacker, J., and Ziebuhr, W. (2000) Effect of subinhibitory antibiotic concentrations on polysaccharide intercellular adhesin expression in Biofilm-forming *Staphylococcus epidermidis*. *Antimicrob. Agents Chemother. 44*, 3357–3363.
26. Bajaj, V., Lucas, R. L., Hwang, C., and Lee, C. A. (1996) Coordinate regulation of *Salmonella typhimurium* invasion genes by environmental and regulatory factors is mediated by control of *hilA* expression. *Mol. Microbiol. 22*, 703–714.
27. Basso, H., Rharbaoui, F., Staendner, L. H., Medina, E., Garcia-Del Portillo, F., and Guzman, C. A. (2002) Characterization of a novel intracellularly activated gene from *Salmonella enterica serovar typhi*. *Infect. Immun. 70*, 5404–5411.
28. Leclerc, G. J., Tartera, C., and Metcalf, E. S. (1998) Environmental regulation of *Salmonella typhi* invasion-defective mutants. *Infect. Immun. 66*, 682–691.
29. Tartera, C., and Metcalf, E. S. (1993) Osmolarity and growth phase overlap in regulation of *Salmonella typhi* adherence to and invasion of human intestinal cells. *Infect. Immun. 61*, 3084–3089.
30. Lamark, T., Rokenes, T. P., McDougall, J., and Strom, A. R. (1996) The complex bet promoters of *Escherichia coli*: regulation by oxygen (ArcA), choline (BetI), and osmotic stress. *J. Bacteriol. 178*, 1655–1662.
31. Rokenes, T. P., Lamark, T., and Strom, A. R. (1996) DNA-binding properties of the BetI repressor protein of *Escherichia coli*: the inducer choline stimulates BetI-DNA complex formation. *J. Bacteriol. 178*, 1663–1670.
32. Ko, R., Smith, L. T., and Smith, G. M. (1994) Glycine betaine confers enhanced osmotolerance and cryotolerance on *Listeria monocytogenes*. *J. Bacteriol. 176*, 426–431.
33. Smith, L. T. (1996) Role of osmolytes in adaptation of osmotically stressed and chill- stressed *Listeria monocytogenes* grown in liquid media and on processed meat surfaces. *Appl. Environ. Microbiol. 62*, 3088–3093.
34. Bayles, D. O., and Wilkinson, B. J. (2000) Osmoprotectants and cryoprotectants for *Listeria monocytogenes*. *Lett Appl. Microbiol. 30*, 23–27.
35. Sakamoto, A., and Murata, N. (2001) The use of bacterial choline oxidase, a glycinebetaine-synthesizing enzyme, to create stress-resistant transgenic plants. *Plant Physiol. 125*, 180–188.
36. Ikuta, S., Imamura, S., Misaki, H., and Horiuti, Y. (1977) Purification and characterization of choline oxidase from *Arthrobacter globiformis*. *J. Biochem. (Tokyo) 82*, 1741–1749.
37. Yamada, H., Mori, N., and Tani, Y. (1979) properties of choline oxidase of *Cylyndrocarpon didymum* M-1. *Agric. Biol. Chem. 43*, 2173–2177.
38. Ohta-Fukuyama, M., Miyake, Y., Emi, S., and Yamano, T. (1980) Identification and properties of the prosthetic group of choline oxidase from *Alcaligenes* sp. *J. Biochem. (Tokyo) 88*, 197–203.
39. Perrino, L. A., and Pierce, S. K. (2000) Choline dehydrogenase kinetics contribute to glycine betaine regulation differences in chesapeake bay and atlantic oysters. *J. Exp. Zool. 286*, 250–261.
40. Perrino, L. A., and Pierce, S. K. (2000) Betaine aldehyde dehydrogenase kinetics partially account for oyster population differences in glycine betaine synthesis. *J. Exp. Zool. 286*, 238–249.
41. Velasco-Garcia, R., Mujica-Jimenez, C., Mendoza-Hernandez, G., and Munoz-Clares, R. A. (1999) Rapid purification and properties of betaine aldehyde dehydrogenase from *Pseudomonas aeruginosa*. *J. Bacteriol. 181*, 1292–1300.
42. Ghanem, M., Fan, F., Francis, K., and Gadda, G. (2003) Spectroscopic and kinetic properties of recombinant choline oxidase from *Arthrobacter globiformis*. *Biochemistry 42*, 15179–15188.
43. Tsuge, H., Nakano, Y., Onishi, H., Futamura, Y., and Ohashi, K. (1980) A novel purification and some properties of rat liver mitochondrial choline dehydrogenase. *Biochim. Biophys. Acta 614*, 274–284.
44. Russell, R., and Scopes, R. K. (1994) Use of hydrophobic chromatography for purification of the membrane- located choline dehydrogenase from a *Pseudomonas* strain. *Bioseparation 4*, 279–284.
45. Fan, F., Ghanem, M., and Gadda, G. (2004) Cloning, sequence analysis, and purification of choline oxidase from *Arthrobacter globiformis*: a bacterial enzyme involved in osmotic stress tolerance. *Arch. Biochem. Biophys. 421*, 149–158.
46. Gadda, G., Powell, N. L., and Menon, P. (2004) The trimethylammonium headgroup of choline is a major determinant for substrate binding and specificity in choline oxidase. *Arch. Biochem. Biophys. 430*, 264–273.
47. Fan, F., and Gadda, G. (2005) On the catalytic mechanism of choline oxidase. *J. Am. Chem. Soc. 127*, 2067–2074.
48. Fan, F., and Gadda, G. (2005) Oxygen- and temperature-dependent kinetic isotope effects in choline oxidase: correlating reversible hydride transfer with environmentally enhanced tunneling. *J. Am. Chem. Soc. 127*, 17954–17961.
49. Ghanem, M., and Gadda, G. (2005) On the catalytic role of the conserved active site residue His466 of choline oxidase. *Biochemistry 44*, 893–904.
50. Fan, F., Germann, M. W., and Gadda, G. (2006) Mechanistic studies of choline oxidase with betaine aldehyde and its isosteric analogue 3,3-dimethylbutyraldehyde. *Biochemistry 45*, 1979–1986.
51. Gadda, G., Fan, F., and Hoang, J. V. (2006) On the contribution of the positively charged headgroup of choline to substrate binding and catalysis in the reaction catalyzed by choline oxidase. *Arch. Biochem. Biophys. 451*, 182–187.
52. Ghanem, M., and Gadda, G. (2006) Effects of reversing the protein positive charge in the proximity of the flavin N(1) locus of choline oxidase. *Biochemistry 45*, 3437–3447.
53. Fan, F., and Gadda, G. (2007) An internal equilibrium preorganizes the enzyme-substrate complex for hydride tunneling in choline oxidase. *Biochemistry 46*, 6402–6408.
54. Quaye, O., Lountos, G. T., Fan, F., Orville, A. M., and Gadda, G. (2008) Role of Glu312 in binding and positioning of the substrate for the hydride transfer reaction in choline oxidase. *Biochemistry 47*, 243–256.
55. Rungsrisuriyachai, K., and Gadda, G. (2008) On the role of histidine 351 in the reaction of alcohol oxidation catalyzed by choline oxidase. *Biochemistry 47*, 6762–6769.
56. Hoang, J. V., and Gadda, G. (2007) Trapping choline oxidase in a nonfunctional conformation by freezing at low pH. *Proteins 66*, 611–620.
57. Schowen, K. B., and Schowen, R. L. (1982) Solvent Isotope Effects on Enzyme Systems, in *Methods Enzymol.* (Purich, D. L., Ed.) pp 551−606, Academic Press, New York.
58. Lide, D. R. (2000) Handbook of Chemistry and Physics, pp 8−57, CRC Press, Boca Raton, FL.
59. Stanislava Kirini, C. K. (1999) Viscosity of aqueous solutions of poly(ethylene glycol)s at 298.15 K. *Fluid Phase Equilib. 155*, 311–325.
60. Cha, S. (1968) A simple method for derivation of rate equations for enzyme-catalyzed reactions under the rapid equilibrium assumption or combined assumptions of equilibrium and steady state. *J. Biol. Chem. 243*, 820–825.
61. Frederick, K. K., and Palfey, B. A. (2005) Kinetics of proton-linked flavin conformational changes in p-hydroxybenzoate hydroxylase. *Biochemistry 44*, 13304–13314.
62. Massey, V., and Ganther, H. (1965) On the interpretation of the absorption spectra of flavoproteins with special reference to D-amino acid oxidase. *Biochemistry 4*, 1161–1173.
63. De Francesco, R., and Edmondson, D. E. (1988) pKa values of the 8 alpha-imidazole substituents in selected flavoenzymes containing 8 alpha-histidylflavins. *Arch. Biochem. Biophys. 264*, 281–287.
64. De Francesco, R., Tollin, G., and Edmondson, D. E. (1987) Influence of 8 alpha-imidazole substitution of the FMN cofactor on the rate of electron transfer from the neutral semiquinones of two flavodoxins to cytochrome c. *Biochemistry 26*, 5036–5042.
65. Williamson, G., and Edmondson, D. E. (1985) Effect of pH on oxidation-reduction potentials of 8 alpha-N-imidazole-substituted flavins. *Biochemistry 24*, 7790–7797.
66. Fersht, A. (1999) Chemical Catalysis, in *Structure and Mechanism in Protein Science* (M.R., J., Ed.) pp 79−84, W. H. Freeman and Company, New York.

BI801424P